DOI: 10.1002/ejic.200900625

Rational Synthesis, Structure, Magnetism and Electrochemistry of Mixed Iron–Nickel-Containing Wells–Dawson-Fragment-Based Sandwich-Type Polyoxometalates

Israel M. Mbomekalle,*[a] Pierre Mialane,[a] Anne Dolbecq,[a] Jérôme Marrot,[a] Francis Sécheresse,[a] Patrick Berthet,[b] Bineta Keita,[c] and Louis Nadjo[c]

Keywords: Polyoxometalates / Sandwich complexes / Nickel / Iron / Magnetic properties / Electrochemistry

The compound $[Na_2(H_2O)_2Ni_2(As_2W_{15}O_{56})_2]^{18-}$, Ni2As4, was synthesized and structurally characterized for the first time by X-ray crystallography. This complex reacts with Fe^{III} to form two new mixed-metal sandwich-type complexes, $[Fe_2(H_2O)_2Ni_2(As_2W_{15}O_{56})_2]^{14-}$, Fe2_Ni2As4, and $[Fe(H_2O)Ni(H_2O)Ni_2(As_2W_{15}O_{56})_2]^{15-}$, FeNi_Ni2As4. In comparison, the synthesis of the previously reported complex $[Na_2(H_2O)_2Fe_2(As_2W_{15}O_{56})_2]^{16-}$, Fe2As4, was rationalized and improved, and the incorporation of Ni^{II} into the latter compound leads to the new mixed-metal complex $[Ni_2(H_2O)_2Fe_2(As_2W_{15}O_{56})_2]^{14-}$, Ni2_Fe2As4. Complete characterization of these complexes by FTIR, UV/Vis, elemental analysis, magnetic measurements and X-ray crystallography, wherever possible, clearly defined their electronic and structural properties. These complexes undergo multiple electron-transfer processes and are effective in the electrocatalytic reduction of nitrite, dioxygen and hydrogen peroxide.

Introduction

Polyoxometalates (POMs) constitute a rapidly growing class of molecular metal–oxygen clusters with applications in catalysis, medicine and molecular magnetism.[1–8] Incorporation of multiple transition-metal ions in lacunary polyoxoanion fragments can lead to transition-metal-substituted polyoxometalates (TMSPs) species with various stoichiometries and structural features. Among this family of TMSPs, sandwich-type complexes constitute a very interesting class due to the number (2, 3, 4 or 6) and the nature of the metal centres that could be included between 2 or 3 multivacant POM fragments.[9–46] Within this class of polyoxoanions, those species based on trivacant Wells–Dawson fragments are particularly attractive. The first Wells–Dawson derivatives, $[M_4(OH_2)_2(P_2W_{15}O_{56})_2]^{16-}$ (M = Co^{2+}, Cu^{2+}, Zn^{2+})[11] was reported by Finke et al. in 1983. Several years later, Bi et al. described the first arsenic(V) analogues of the Wells–Dawson type, $[M_4(OH_2)_2(As_2W_{15}O_{56})_2]^{16-}$ (M = Mn^{II}, Co^{II}, Ni^{II}, Cu^{II}, Zn^{II}, Cd^{II}).[28a] These two families of complexes can be considered as "saturated", as they have in their structure the maximum number of d metal centres that can be "sandwiched" by the trivacant Wells–Dawson polyoxoanion $[X_2W_{15}O_{56}]^{12-}$ (X = As or P). Therefore, no further addition of a new metal centre (identical or different) can occur.

The first example of a sandwich-type species with less than four transition metals was described by Hill et al.[30] The diiron(III)-substituted polyanion $[(NaOH_2)_2Fe_2(P_2W_{15}O_{56})_2]^{16-}$ is based on two Wells–Dawson fragments $[P_2W_{15}O_{56}]^{12-}$ that sandwich a tetranuclear metal cluster, $[Fe_2O_{14}(NaOH_2)_2]$, in which the two equivalent interior positions are occupied by Fe^{III} centres, and the two equivalent exterior positions are occupied by sodium ions in the solid state. It was also shown that this polyanion reacts with Cu^{2+} or Co^{2+} ions in aqueous solution, leading to a trisubstituted mixed-metal sandwich-type polyanion[31] with partial decomposition of one of the $[X_2W_{15}O_{56}]^{12-}$ fragments (two tungsten atoms nearest the vacant site in the central unit are now replaced by Cu or Co atoms).

Since then, many reports have surfaced based on mixed-metal sandwich-type complexes. For example, the addition of several divalent "d" metal cations on $[(NaOH_2)_2Fe_2(X_2W_{15}O_{56})_2]^{16-}$ (X = As or P) under mild conditions leads to mixed-metal complexes $[(MOH_2)_2Fe_2(X_2W_{15}O_{56})_2]^{16-}$, where M = Ni^{II}, Mn^{II}, Co^{II} or Zn^{II} and X = As or

[a] Institut Lavoisier de Versailles, UMR 8180, CNRS Université de Versailles Saint-Quentin,
45 Avenue des Etats-Unis, 78035 Versailles Cedex, France
Fax: +33-1-39254452
E-mail: israel.mbomekalle@chimie.uvsq.fr
[b] Laboratoire de Physico-Chimie de l'Etat Solide, ICMMO, UMR 8182, CNRS, Université Paris-Sud, Bâtiment 410,
91405 Orsay Cedex, France
[c] Laboratoire de Chimie Physique, UMR 8000, CNRS, Electrochimie et Photoélectrochimie, Université Paris-Sud, Bâtiment 350,
91405 Orsay Cedex, France

Supporting information for this article is available on the WWW under http://dx.doi.org/10.1002/ejic.200900625.

P.[33,37,38,41] More recently, addition of one d metal cation on trisubstituted, sandwich-type polyoxoanions $[(NaOH_2)(MOH_2)M_2(P_2W_{15}O_{56})_2]^{17-}$, where M = Mn^{II} or Co^{II} was described.[43] The first example of a mixed-metal sandwich-type complex described by Wasfi et al. in 1987[13] proceeded by a one-pot synthesis and contained two different d metal centres in its central cluster.

These compounds are of great importance, as their properties can be finely tuned by changing the number and/or nature of elements "sandwiched" in the metal cluster. In line with the studies we have undertaken for a few years now,[47] we are developing simple and rational procedures that may improve targeted syntheses of new POMs likely to play a major role in catalytic and electrocatalytic reactions.[48] In fact, it was found that the location, nature and number of the d metal centres in the POM framework may influence the interactions between redox-active centres within the molecule. For example, the catalytic efficiency of Fe^{III}-containing sandwich-type complexes $[Fe_y(X_2W_{15}O_{56})_2]^{n-}$ (where X = As or P and y = 2, 3 or 4) towards the electroreduction of dioxygen is improved when the number of Fe atoms is increased.[49] Another illustration of the influence of active d metal centres is the cooperative effect of Mn^{II} and Fe^{II} centres in the electrocatalytic reduction of nitrogen oxides.[49] It is well established that Fe^{III}-substituted POMs catalyze the reduction of NO and/or NO_2^-.[50–53] The presence of two manganese atoms in the compound $[(MnOH_2)_2Fe_2(X_2W_{15}O_{56})_2]^{16-}$ (X = As or P) stabilizes this complex and thus enhances the catalytic efficiency towards the reduction of nitrite.[49]

One of the remaining challenges is to master the spatial distribution of metal centres within the central cluster in mixed-metal sandwich-type POMs. It is anticipated that new electrochemical and electrocatalytic behaviours might ensue.

Here we report on some novel polyoxoanions that were obtained as results of our research efforts along these directions. The compound $[(NaOH_2)_2Ni_2(As_2W_{15}O_{56})_2]^{18-}$ (abbreviated Ni2As4 in the following), in which the nickel centres occupy the so-called interior positions, was synthesized and structurally characterized for the first time by X-ray crystallography. This complex reacts with Fe^{III} to form two new mixed-metal sandwich-type complexes, $[Fe_2(OH_2)_2Ni_2(As_2W_{15}O_{56})_2]^{14-}$ (abbreviated Fe2_Ni2As4) and $[Fe(OH_2)Ni(OH_2)Ni_2(As_2W_{15}O_{56})_2]^{15-}$ (abbreviated FeNi_Ni2As4). For comparison, the new mixed-metal complex $[Ni_2(OH_2)_2Fe_2(As_2W_{15}O_{56})_2]^{14-}$ (abbreviated Ni2_Fe2As4) was obtained by starting from the previously reported complex $[Na_2(OH_2)_2Fe_2(As_2W_{15}O_{56})_2]^{16-}$ (abbreviated Fe2As4), the synthesis of which was also rationalized and improved.

Thus, the possibilities for the two Fe centres in $[M_2Fe_2(X_2W_{15}O_{56})_2]^{16-}$ (X = As or P)-type complexes, to be fixed, at will, in the internal or the external positions are opened.

Complete characterization of these complexes by FTIR, UV/Vis, elemental analysis, magnetic measurements and X-ray crystallography, wherever possible, clearly defined their electronic and structural properties. Electrochemistry shows that these complexes undergo multiple electron-transfer processes and are effective in the electrocatalytic reduction of nitrite, dioxygen and hydrogen peroxide.

Results and Discussion

Syntheses

The synthetic procedure developed in the present study was adapted from the one described by Ciabrini and Contant.[54] Complexes $[Na_2(H_2O)_2M_2(X_2W_{15}O_{56})_2]^{n-}$ (M = Cr^{III}, Mn^{II}, Co^{II}, Ni^{II}, Cu^{II}, Zn^{II} and X = As or P) were obtained pure, in good yields (60–90%). To the best of our knowledge, this is the first time that dinuclear Wells–Dawson sandwich-type complexes have been obtained in a single step, with no byproduct. In previously described procedures, several steps were necessary to get pure samples of the dinuclear complex $M_2(X_2W_{15}O_{56})_2$ free from the tri- and tetranuclear parent products $M_3(X_2W_{15}O_{56})_2$ and $M_4(X_2W_{15}O_{56})_2$.[32] The key to our success was the combined effect of Na^+ ions and the pH of the medium, ca. 4.6 (acetate buffer). These two factors lead to a better stabilization of the trilacunary species $[X_2W_{15}O_{56}]^{12-}$ (X = As or P).[7,56] Furthermore, slow addition of a molar equivalent of the corresponding metallic salt to the solution containing the lacunary species favoured the formation of the sandwich-type complex containing only two first-row "d" metal centres.

The same method was used to prepare the iron(III)-substituted complex $[Na_2(H_2O)_2Fe^{III}_2(As_2W_{15}O_{56})_2]^{16-}$[37] (see Supporting Information). Similar results were obtained when $[P_2W_{15}O_{56}]^{12-}$ was used instead of $[As_2W_{15}O_{56}]^{12-}$. A comprehensive and comparative study of this family of Wells–Dawson sandwich-type complexes, confirming and completing published work,[37,41,49] has been done and will be published later.

Several reactions of d-block transition metals with $[(NaOH_2)_2Fe^{III}_2(X_2W_{15}O_{56})_2]^{16-}$ (where X = As or P) have been widely reported.[31,33,41] The common feature of these compounds described up to now is that Fe^{III} centres are always located on the internal sites of the equatorial metal cluster $Fe_2O_{14}(MOH_2)_2$. Here we developed a rational addition of Fe^{III} to a well-characterized dinuclear sandwich-type complex $[(NaOH_2)_2Ni^{II}_2(As_2W_{15}O_{56})_2]^{18-}$. Under controlled experimental conditions, this addition leads to two different mixed-metal sandwich-type complexes, $[Fe_2(OH_2)_2Ni_2(As_2W_{15}O_{56})_2]^{14-}$, (abbreviated Fe2_Ni2As4) and $[Fe(OH_2)Ni(OH_2)Ni_2(As_2W_{15}O_{56})_2]^{15-}$ (abbreviated FeNi_Ni2As4), which were identified and unambiguously characterized by elemental analysis, magnetic measurements and electrochemistry. In these complexes, the Fe^{III} centres are located in the external sites of the median cluster, whereas the Ni^{II} centres are located in the internal sites. This is the first time, to the best of our knowledge, that such a mixed-metal sandwich-type complex is reported.[55]

Addition of Ni^{II} to Fe2As4 leads, as expected, to Ni2_Fe2As4, where the external positions in the central tetranuclear cluster are occupied by the nickel atoms as observed

for $[M_2(H_2O)_2Fe_2(As_2W_{15}O_{56})_2]^{14-}$ (M = Mn and Zn).[37,41] Its phosphorus analogue, $[Ni_2(H_2O)_2Fe_2(P_2W_{15}O_{56})_2]^{14-}$, has been described by Hill et al.[33]

Summarizing, we have obtained three different mixed-metal Wells–Dawson sandwich-type complexes: the first one, Fe2_Ni2As4, in which the two nickel atoms occupy the internal positions of the central metal cluster and the iron atoms the external ones. Each Fe^{III} is coordinated to a single water molecule. In the second complex, FeNi_Ni2As4, one of the external Fe atoms is replaced by a nickel atom. The third complex, Ni2_Fe2As4, has exactly the same atoms in the central cluster as the first one, but their positions differ: here the Fe atoms are internal and the Ni atoms, each coordinated by one H_2O molecule, are external. As a comparison, the parent complexes Ni4As4, Ni2As4 and Fe2As4 are included in the discussion when necessary.

Structures

As the Ni4As4 and Ni2_Fe2As4 complexes form the $[(NiOH_2)_2M_2(As_2W_{15}O_{56})_2]$ (M = Ni^{II}, Fe^{III}) sandwich-type POM structures already described with phosphotungstate Wells–Dawson precursors,[23,33] their crystal structures have not been studied. On the contrary, no X-ray structure of a dinuclear divalent sandwich-type complex has been reported even if the structure of the $[(NaOH_2)_2Co^{II}_2(P_2W_{15}O_{56})_2]^{18-}$ POM has been postulated on the basis of ^{31}P NMR spectroscopy and electrochemistry.[32b] The X-ray crystal structure of Ni2As4 has then been studied and reveals a lacunary sandwich-type structure $[(NaOH_2)_2Ni^{II}_2(As_2W_{15}O_{56})_2]^{18-}$ in which the outer sites of the M_4O_{16} unit are occupied by sodium ions (Figure 1 and Table 1). In Ni2As4, the two sodium ions located in the belt adopt an octahedral coordination, being connected to five oxo ligands of the POM (average Na–O bond length 2.31 Å) and one terminal water molecule (2.40 Å). The Ni^{II} ions are also hexacoordinate, with Ni–O bond lengths in the 1.780(13)–2.061(12) Å range (see Table 2).

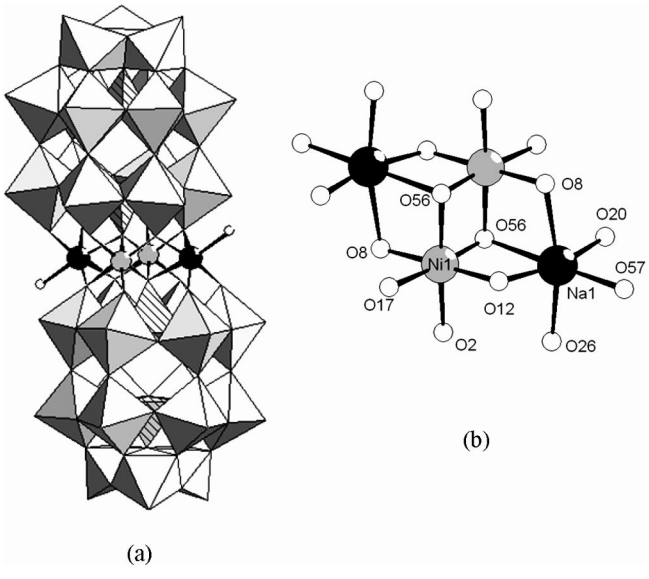

Figure 1. (a) Mixed ball-and-stick and polyhedral representation of the polyanion in Ni2As4. White octahedra, WO_6; hatched tetrahedra AsO_4; light grey spheres, Ni; black spheres, Na; white spheres, O. (b) Atom labelling scheme of the central M_4O_{16} unit.

Table 1. Crystallographic data for Ni2As4 and Fe0.5Ni_Ni2As4.

	Ni2As4	Fe0.5Ni_Ni2As4
Empirical formula	$H_{86}As_4Na_{20}Ni_2O_{155}W_{30}$	$H_{104}As_4Fe_{0.5}Na_{15.5}Ni_3O_{165}W_{30}$
Formula weight / g	8959.09	9119.58
Crystal system	monoclinic	triclinic
Space group	$P2_1/c$	$P\bar{1}$
a / Å	17.063(3)	13.677(4)
b / Å	15.114(3)	13.904(4)
c / Å	32.217(7)	23.101(7)
α / °	90	90.04(1)
β / °	91.532(7)	101.91(1)
γ / °	90	118.41(1)
V / Å^3	8305(3)	3756(1)
Z	2	1
T / K	293	100
ρ_{calcd} / g cm^{-3}	3.582	3.986
μ / mm^{-1}	21.852	24.322
Data/parameters	24235/897	36937/1604
R_{int}	0.0776	0.0431
GOF	1.035	1.101
R [$>2\sigma(I)$]	R_1 = 0.0587	R_1 = 0.0389
	wR_2 = 0.1511	wR_2 = 0.1029

Table 2. Selected bond lengths [Å] in Ni2As4 and Fe0.5Ni_Ni2As4 associated to the representations of Figures 1 and 2.

Ni2As4			
Ni1–O56	1.780(13)	Na1–O12	2.012(11)
Ni1–O56	2.041(11)	Na1–O20	2.074(14)
Ni1–O17	2.042(10)	Na1–O26	2.255(14)
Ni1–O2	2.051(11)	Na1–O57	2.355(22)
Ni1–O12	2.056(11)	Na1–O8	2.356(13)
Ni1–O8	2.061(12)	Na1–O56	2.408(13)
Fe0.5Ni_Ni2As4			
Ni1–O51	1.964(19)	Ni2–O44	1.98(2)
Ni1–O55	2.00(2)	Ni2–O112	2.019(19)
Ni1–O101	2.02(2)	Ni2–O113	2.05(2)
Ni1–O105	2.11(2)	Ni2–O48	2.05(2)
Ni1–O113	2.11(2)	Ni2–O56	2.10(2)
Ni1–O56	2.16(2)	Ni2–O108	2.150(18)
Ni3–O36	1.986(32)	Na1–O57	1.85(3)
Ni3–O41	2.005(32)	Na1–O98	2.06(3)
Ni3–O114	2.007(32)	Na1–O93	2.11(14)
Ni3–O108	2.018(29)	Na1–O51	2.28(3)
Ni3–O105	2.059(30)	Na1–O48	2.30(3)
Ni3–O56	2.078(27)	Na1–O113	2.54(3)
Fe1–O93	2.06(3)	Fe1–O98	2.14(2)
Fe1–O113	2.10(2)	Fe1–O51	2.19(2)
Fe1–O48	2.11(2)	Fe1–O57	2.29(3)

A crystal of the recrystallized FeNi_Ni2As4 has also been studied by X-ray diffraction. Its structure can be solved in the centrosymmetric space group $P\bar{1}$ like most of the sandwich-type compounds, as illustrated by the X-ray determination of Ni2As4. However, in this space group, a disorder is observed between the Ni^{II} and Fe^{III} ions on the outer positions. Therefore we have forced the resolution in the noncentrosymmetric space group $P1$. In $P1$, the four paramagnetic atoms are crystallographically independent.

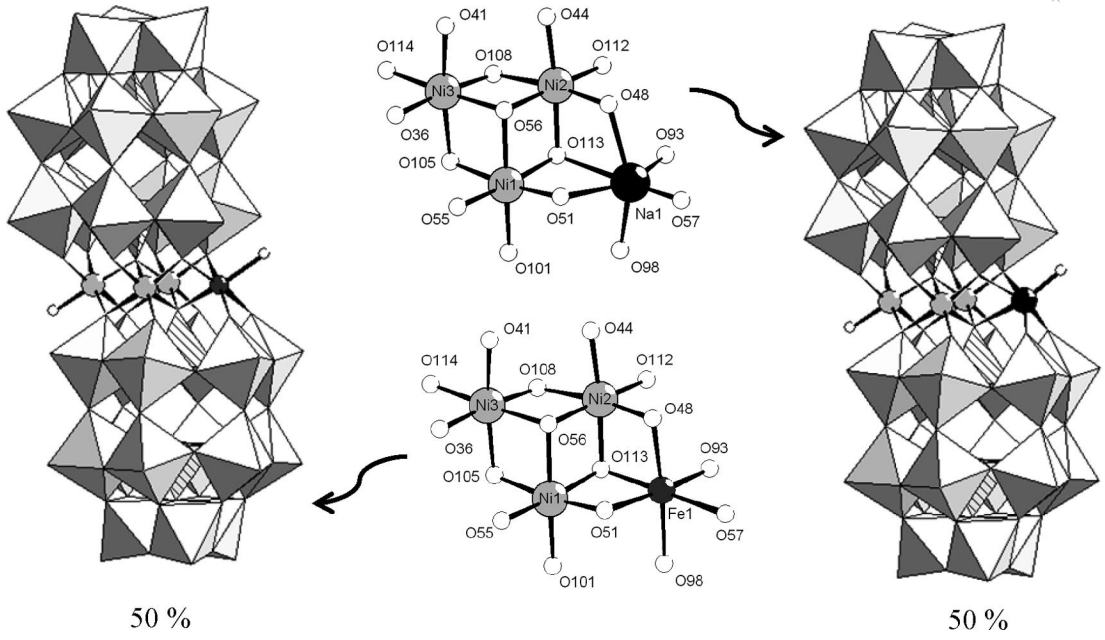

Figure 2. Mixed ball-and-stick and polyhedral representations of the polyanion and atom labelling scheme of its central M_4O_{16} unit in Fe0.5Ni_Ni2As4, showing the disorder between the iron ion and the sodium ion in the central belt. White octahedra, WO_6; hatched tetrahedra AsO_4; light grey spheres, Ni; black sphere, Na; white spheres, O, medium grey sphere, Fe.

As expected, the two Ni^{II} ions located in the Ni2As4 precursor are also found in the inner positions with Ni–O distances in the 1.96(2)–2.16(2) Å range. A third Ni^{II} cation is found on one of the outer positions. Valence-bond calculations[57] confirm the divalent character of this ion (Σs = 2.06), with an average Ni–O distance of 2.03 Å. The Fe^{III} centre is found on the second outer position. Nevertheless, the resolution of the structure is improved when a disorder between this Fe^{III} ion and a sodium ion is considered, with half occupancy factors (Figure 2). This compound has thus been named Fe0.5Ni_Ni2As4. The partial substitution of the Fe^{III} ion by a sodium cation is probably due to the recrystallization steps needed to obtain a single crystal of suitable quality for single-crystal X-ray diffraction studies and confirms the instability of this species (see below).

Magnetic Studies

The temperature dependence of the magnetization was studied in a 0.1 T field from 2 or 5 K to 250 K. In the particular case of the Fe2As4 compound a paramagnetic contribution attributed to free Fe^{3+} impurities was subtracted from the raw data before further treatment; this contribution represents less than 3% of the iron atoms of the sample under study. As it appears quite convenient to reveal the specific behaviour of each compound, the value of the $\chi_{mol}T$ product was then calculated from the experimental data and plotted as a function of the temperature in Figure 3. For all the compounds containing nickel ions, the $\chi_{mol}T$ product exhibits a maximum found between 2.5 and 10 K. The existence of this maximum is a first indication of the predominance of ferromagnetic interactions between the magnetic ions forming the central cluster coupled to antiferromagnetic interactions between neighbour clusters or the zero-field splitting (ZFS) effect. The temperature dependence of the $\chi_{mol}T$ product of the Fe2As4 compound is quite different, as it decreases regularly with T, which indicates an antiferromagnetic interaction between the two iron atoms. To carry out a quantitative analysis of the magnetic interactions, the experimental susceptibility of the complexes under study was written as:

$$\chi_{mol} = [T/(T - T_{CW})\chi_{cluster}] + \chi_0$$

where T_{CW} is the negative Curie–Weiss temperature accounting for the mean field corrections associated to antiferromagnetic intercluster interactions and ZFS, χ_0 represents temperature-independent contributions and $\chi_{cluster}$ the intrinsic susceptibility of the cluster. The χ_0 value is mainly due to the diamagnetism of the ligands and of the sample holder but for cluster-containing nickel ions, temperature-independent paramagnetism may also occurred. The $\chi_{cluster}$ value is given by the following equation:

$$\chi_{cluster} = g^2N\beta^2 <S_T(S_T + 1)>/3kT$$

in which the mean value $<S_T(S_T + 1)>$ depends on the temperature, which determines the population of the energy levels resulting from the individual spin coupling. These energy levels are eigenvalues of the magnetic Hamiltonian of the cluster. For the polyanions under study, the more general Hamiltonian is that describing tetranuclear clusters, however, those related to dinuclear clusters may be easily deduced from it by setting the spin value of two of the four ions to zero.

As the magnetic ions of the tetranuclear clusters are found at the corners of an almost regular rhomboid, the magnetic interactions can be represented by two exchange constants, J_1 and J_2, describing, respectively, the interactions along the sides of the rhomboid and that along its

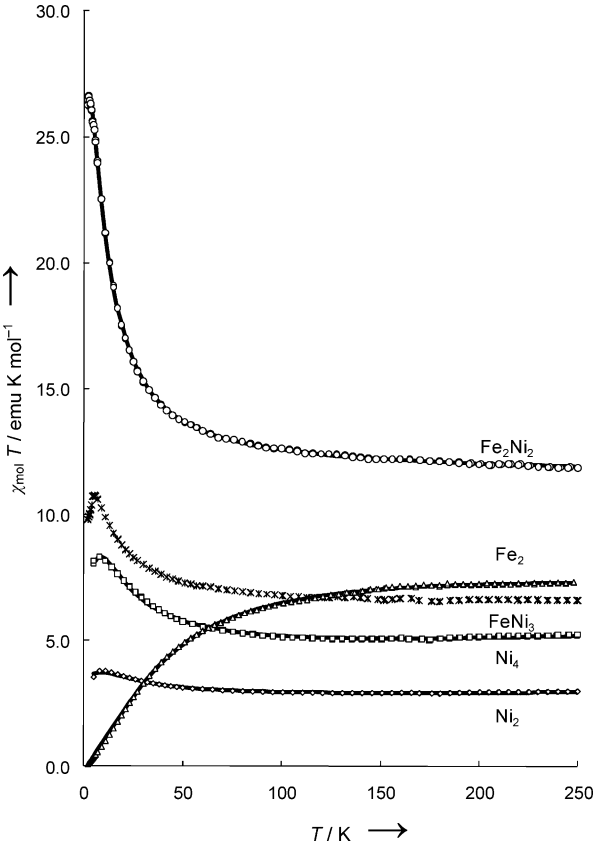

Figure 3. Plot of the $\chi_{mol}T$ product as a function of temperature for the Ni2As4, Ni4As4, FeNi_Ni2As4, Fe2As4 and Fe2_Ni2As4 compounds identified by the magnetic ions comprised in their central cluster. The symbols represent the experimental data and the continuous lines the least-square fits using the parameters reported in Table 3.

shortest diagonal except in the case of the $FeNi_3$ cluster, which exhibits two different types of sides and cannot be analyzed with the following method. These interactions are of the superexchange type; they are mediated by two bridging oxygen ions forming the edge shared by two neighbouring MO_6 octahedra (M = Fe, Ni). Therefore, the magnetic energy of the cluster can be described by the following Heisenberg-type Hamiltonian:

$$\hat{H} = -2J_1(\hat{S}_1\hat{S}_2 + \hat{S}_2\hat{S}_3 + \hat{S}_3\hat{S}_4 + \hat{S}_4\hat{S}_1) - 2J_2\hat{S}_1\hat{S}_3$$

The eigenvalues of this Hamiltonian operator are obtained by the vector-coupling method of Kambe:[58]

$$E_i(S_T,S_{13},S_{24}) = -J_1[S_T(S_T + 1) - S_{13}(S_{13} + 1) - S_{24}(S_{24} + 1)] - J_2[S_{13}(S_{13} + 1) - S_1(S_1 + 1) - S_3(S_3 + 1)]$$

where S_{13}, S_{24} and S_T are related with the spin operators $\hat{S}_{13} = \hat{S}_1 + \hat{S}_3$, $\hat{S}_{24} = \hat{S}_2 + \hat{S}_4$ and $\hat{S}_T = \hat{S}_{13} + \hat{S}_{24}$.

The number of (S_T,S_{13},S_{24}) combinations of energy E_i depends on the number of magnetic ions in the cluster and of their spins. There are respectively 46, 19, 6 and 3 combinations for the Fe_2Ni_2, Ni_4, Fe_2 and Ni_2 clusters. After the calculation of these energies, the mean value of $<S_T(S_T + 1)>$ is obtained as:

$$<S_T(S_T + 1)> = \Sigma\, a_i\exp(-E_i/kT)/\Sigma b_i\exp(-E_i/kT)$$

with $b_i = 2S_T(E_i) + 1$ and $a_i = b_iS_T(E_i)[S_T(E_i) + 1]$.

By fitting the calculated $\chi_{mol}T$ values to the experimental ones, it is possible to determine the magnetic parameters describing the cluster (Table 3). The examination of the parameters reported in Table 3, confirms the antiferromagnetic nature of the interactions ($J_2 < 0$) between the iron ions in the Fe2As4 compound, whereas all the other internal interactions are ferromagnetic. For the Fe_2Ni_2 and the Ni_4 tetranuclear clusters the ferromagnetic interaction is stronger along the short diagonal of the rhomboid (J_2) than along its sides (J_1). For the first compound, J_1 describes Fe–Ni interactions, whereas J_2 describes Ni–Ni interactions; therefore, the difference between J_1 and J_2 may have mainly a chemical origin. For the second compound this difference reflects those existing between the Ni–O–Ni angles and between the Ni–O distances. The data previously reported for analogous compounds clearly indicate that the Ni–Ni interactions are very sensitive to the geometry of the cluster: in contrast with the present result, J_1 is found larger than J_2 in Ni_4 clusters encapsulated in phosphorus derivatives,[19,23] whereas J_1 is found equal to J_2 in the corresponding Ni_3 cluster.[19,36] Moreover, a negative value of J_2 has already been observed for a Ni_3 cluster.[36]

Table 3. Magnetic parameters and first energy levels of the compounds under study.

	Ni2As4	Ni4As4	Fe2As4	Fe2_Ni2As4
g	2.27	2.00	2.03	2.08
J_1 / cm^{-1}	–	2.81	–	0.91
J_2 / cm^{-1}	6.18	9.75	–2.94	6.62
X_0 / emu mol^{-1}	0.97×10^{-3}	3.62×10^{-3}	-0.33×10^{-3}	-0.34×10^{-3}
T_{CW} / K	–0.26	–1.14	0	–0.27
E_0 / cm^{-1} [S_T]	–12.4 [2]	–42.0 [4]	–51.4 [0]	–31.4 [7]
E_1 / cm^{-1} [S_T]	12.4 [1]	–30.7 [3]	–45.6 [1]	–27.8 [6]

The ground-state energy E_0 always corresponds to the highest possible spin for the nickel-containing clusters as expected the ferromagnetic nature of all the interactions, whereas it corresponds to an $S = 0$ spin state for the Fe2As4 compound. For most complexes, the ground state is well separated (more than 5 cm^{-1}) from the first excited state of energy E_1. The values of the temperature-independent susceptibilities χ_0 are quite different from one complex to another and are sometimes positive; as already mentioned, this term results from the competition between several contributions. However, it is clear that Ni4As4 and Ni2As4 exhibit temperature-independent paramagnetism. The Landé g-factors are close to 2 for all the samples; the slight deviations from this value may be due to the distortion of the ion environment or to experimental uncertainties such as the exact molar weights of the compounds that depend on their water contents. Finally, the Curie–Weiss T_{CW} temperatures have values that indicate that the interactions between the ferromagnetic clusters are rather weak.

Stability Studies

Preliminary stability studies in solution as a function of pH (from 1 to 7) were done for all the compounds men-

tioned above. UV/Vis spectra of their solutions were recorded as a function of pH over a period of 24 h. The stability criterion was reproducibility of spectra with respect to absorbance and wavelengths during this period of time. All complexes were found to be stable in solution over the pH range of 1 to 7, except FeNi_Ni2As4, which shows slow decomposition at pH 1. The spectra recorded at pH 3 are shown in the Supporting Information. Complementary confirmation of stability was obtained by electrochemistry: cyclic voltammograms of the given compounds were reproducible after several hours.

Electrochemistry

The cyclic voltammetry (CV) study of the present complexes is restricted to new features compared to previous analogous reports. However, complementary detailed descriptions including studies as a function of pH, can be found in the Supporting Information. A pH 3.00 medium (0.5 M Li_2SO_4 + H_2SO_4) was selected as the main supporting electrolyte. For clarity, emphasis is put on new compounds, including all the Fe-containing derivatives. Comparison of the cyclic voltammograms of Ni4As4 and Ni2As4 shows two successive four-electron redox processes, featuring the reduction of tungsten centres, a behaviour which is typical of Wells–Dawson sandwich-type complexes[59] (see Table 4 and Supporting Information). As expected, the CV of the new compound Fe2_Ni2As4 obtained upon addition of two iron cations onto one molecule of Ni2As4 shows a new redox wave attributed to the Fe^{III}/Fe^{II} couple (Supporting Information).[60] It must be kept in mind that the substitution of two Na^+ ions by two Fe^{III} centres in one molecule of Ni2As4 is accompanied by at least two physical and structural transformations: (1) the overall negative electrical charge of the anion decreases by 4 units[61] and (2) the modification of junctions that exist between the tungsten fragments, $[As_2W_{15}O_{56}]^{12-}$, and the equatorial metallic cluster, $Ni_2M_2O_{14}(OH_2)_2$, with M = Na^+ or Fe^{3+}.[62] Modifications observed on the first tungsten wave (reduction much easier and more pronounced basic character) therefore should be the consequences of these important physical and structural changes.

In addition to details relegated to the Supporting Information, including the comparison of the CVs of Ni2_Fe2As4 and that of its parent compound Fe2As4, all other cross-comparisons can be made from Table 4, which gathers the reduction peak potentials for Fe and W waves determined by cyclic voltammetry at pH 3.00 for the six complexes.

The CVs of the compounds Fe2_Ni2As4 and FeNi_Ni2As4 are compared in Figure 4. The major difference in the pattern can be attributed to Fe^{III}/Fe^{II} couple. The reduction current drops to half its value when passing from Fe2_Ni2As4 to FeNi_Ni2As4 with a slight shift to positive potentials (ca. 14 mV). Controlled potential coulometry experiments conducted at –0.2 V vs. SCE reference electrode on solutions of these two compounds in 1.0 M $LiCH_3COO$ pH 5.00 electrolyte confirmed the presence of one and two atoms of Fe per molecule of FeNi_Ni2As4 and Fe2_Ni2As4, respectively (Supporting Information). It is important to note that the two Fe centres of Fe2_Ni2As4 are reduced in a single step, a feature that differs from the stepwise reduction observed in $[Fe_y(X_2W_{15}O_{56})_2]^{n-}$ (where X = As or P and y = 2, 3 or 4).[48,49] Complementary data can be found in Table S2 and the Supporting Information.

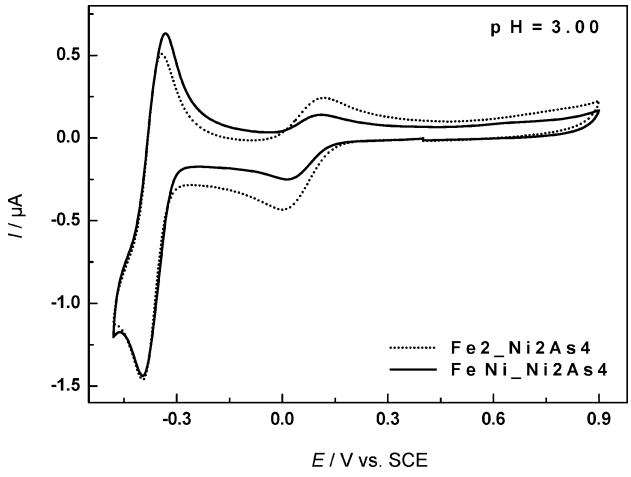

Figure 4. Comparison of the cyclic voltammograms of Fe2_Ni2As4 (dotted line) and FeNi_Ni2As4 (solid line) in a pH 3 medium (0.5 M Li_2SO_4 + H_2SO_4). Polyoxometalate concentration: 0.1 mM; scan rate: 10 mV s^{-1}; working electrode: glassy carbon; reference electrode: SCE.

We now come to the comparison of the CVs of Fe2_Ni2As4 and Ni2_Fe2As4. These two compounds are identical in composition and structure; they only differ in the

Table 4. Reduction peak potential, E_{pc} (V vs. SCE) for Fe and W waves determined by cyclic voltammetry at pH 3.00 (0.5 M Li_2SO_4 + H_2SO_4) for the six complexes. Scan rate: 10 mV s^{-1}, working electrode: glassy carbon.

	E_{pc} (V vs. SCE)			
	Fe	W1	W2	W3
Ni4As4	–	–0.390	–0.602	–0.836
Ni2As4	–	(–0.305)[a] –0.416	–0.548	–0.832
Fe2_Ni2As4	+0.004	–0.398	–0.604	–0.834
FeNi_Ni2As4	+0.018	–0.396	(–0.542)[a] –0.606	–0.832
Fe2As4	–0.098 (–0.202)[b]	(–0.374)[a] –0.436	–0.542	–0.826
Ni2_Fe2As4	–0.052 (–0.158)[b]	–0.404	–0.584	–0.838

[a] Shoulder on the main wave. [b] The reduction of the two Fe atoms occurs in two separate steps.

relative positions of the iron and nickel atoms within the median tetrametallic cluster $[Ni_2Fe_2O_{14}(OH_2)_2]$. Indeed, the Fe^{III} centres of Fe2_Ni2As4 are located in the so-called "external sites", whereas they are located in the so-called "internal sites" in Ni2_Fe2As4 (vide supra). This structural difference turns out to induce different electrochemical behaviours. Two striking differences appear, as concerns both the potential location and the shape of waves featuring the Fe^{III}/Fe^{II} redox process (Supporting Information): there is a gap of approximately 150 mV between the two reduction peak potentials; a single-step reduction of the Fe centres of Fe2_Ni2As4 versus a two-step reduction in Ni2_Fe2As4 will also be discussed in the following. As the compounds have exactly the same electrical charge (–14), no charge consideration can therefore explain the difference in peak potential locations. Experimental and theoretical studies carried out on sandwich-type complexes containing more than two Fe^{III} centres reveal that Fe^{3+} ions centres located in the external sites are always reduced before the ones located in internal sites.[36,49,63,64] However, these studies remain difficult for at least two reasons. Firstly, it is difficult to differentiate easily and without doubt the two types of Fe^{III} centres only on the basis of their electrochemical behaviours. Secondly, relatively strong interactions exist between these close metallic centres. In this context, it is quite difficult to identify and quantify the influence of the first reduction on the second one. In contrast, the complexes of the present work would appear to provide a simple case for the study of redox properties of Fe^{III} centres in external or internal sites because they are associated with nonelectroactive metallic centres. Ni^{II} is not electroactive within the potential domain being explored here and there is no competition between the reduction of Fe^{III} and Ni^{II}. It can be concluded that we have built a unique opportunity to compare electrochemical behaviours, extended to magnetic properties, of external or internal Fe^{III} centres with no interaction of the other adjacent Fe^{III} centres.

Figure 5 presents a comparison of Fe2_Ni2As4 and Ni2_Fe2As4 CVs recorded under the same conditions and restricted to the Fe^{III}/Fe^{II} redox process. We note that the reduction of the external Fe^{III} centres (for Fe2_Ni2As4) proceeds in a single step (+ 40 mV vs. SCE), whereas the reduction of the other two internal ones (for Ni2_Fe2As4) proceed in two steps (–52 and –158 mV vs. SCE). At least two reasons, alone or in combination, might explain the coalescence versus splitting of these waves. The spatial location of the two external iron centres will minimize the interaction between them and maintain their equivalence and independence during reduction processes. The contrary is true for the internal irons. The result is a coalescence of the wave for these two electrons, whereas for internal iron the waves remain clearly composite. Provisionally, it is also worth noting that each external iron is bound to a water molecule that completes its octahedral coordination sphere. This H_2O molecule is a favourable site for protonation. The external iron will, therefore, be subject to a much greater influence of protonation than the internal iron.

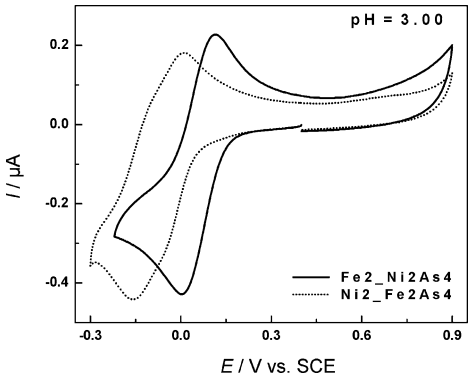

Figure 5. Comparison of cyclic voltammograms of Fe2_Ni2As4 (solid line) and Ni2_Fe2As4 (dotted line) in a pH 3 medium (0.5 M Li_2SO_4 + H_2SO_4). Polyoxometalate concentration: 0.1 mM; scan rate: 10 mV s^{-1}; working electrode: glassy carbon; reference electrode: SCE. Scan restricted to the Fe^{III}/Fe^{II} wave.

pH Influence

Many studies focused on the influence of pH on the electrochemical properties of POMs have proved that redox processes between the working electrode and the POM molecule are generally coupled to an acid reaction (proton exchange) through an electrochemical–chemical (EC) or an electrochemical–chemical–electrochemical (ECE) mechanism. In this section, we describe the electrochemical behaviours of the Fe-containing derivatives. The same details for the other complexes can be found in the Supporting Information. This study is restricted to the three following media: 0.5 M Li_2SO_4 + H_2SO_4 pH 1 and 3 and 1.0 M $LiCH_3COO$ + CH_3COOH pH 5, with a particular emphasis on the behaviours at pH 5.

At pH 1 (0.5 M Li_2SO_4 + H_2SO_4), where FeNi_Ni2As4 is unstable, the comparative study is restricted to the three other iron-substituted compounds, Fe2_Ni2As4, Fe2As4 and Ni2_Fe2As4. Comparison of the CVs run in this medium (Figure 6) reveals the following sequences for the reduction peak potentials and peak current intensities for the Fe^{III}/Fe^{II} redox couple: Ep(Fe2_Ni2As4) > Ep(Ni2_Fe2s4) > Ep(Fe2As4) and Ip(Fe2_Ni2As4) < Ip(Ni2_Fe2As4) < Ip(Fe2As4). The striking feature accompanying these sequences is that the wave associated with the redox process Fe^{III}/Fe^{II} looses some of its "reversibility" when moving from the compound Fe2As4 with no Ni^{II} centres to the compound Ni2_Fe2As4 with two Ni^{II} centres located in the external sites. A large separation between the cathodic and anodic processes is observed for Fe2_Ni2As4, in which the Fe^{III} are located in the external sites and the Ni^{II} centres in the internal sites (see Figure 6). Furthermore, it must be pointed out that the two-electron exchange during the reduction process of the two Fe^{III} centres is realized in a single-step for Fe2_Ni2As4, whereas a two-step process for Fe2As4 and Ni2_Fe2As4 is observed. The wave shapes and relative current intensities would suggest the observed behaviours to be related to a chemical transformation, including acid–base properties of the reduced species of the three complexes rather than to a slowness of the electron transfer

kinetics. The following observation supports such assumption: at pH 3 and pH 5, the Fe^{III}/Fe^{II} redox process in Fe2_Ni2As4 becomes more reversible with peak potential shifts in the negative direction (Supporting Information). This change is linear between pH 1 and pH 5 with an average slope of 87.5 mV/pH.

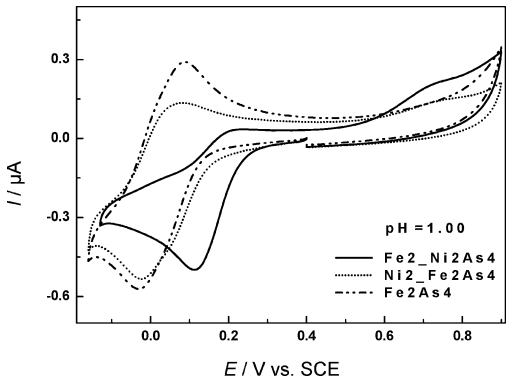

Figure 6. Cyclic voltammograms of Fe2_Ni2As4 (solid line), Ni2_Fe2As4 (dotted line) and Fe2As4 (dashed dotted line) in 0.5 M Li_2SO_4 + H_2SO_4, pH 1.00. The scan is restricted to the redox process of Fe^{III}. Polyoxometalate concentration: 0.1 mM; scan rate: 10 mV s^{-1}; working electrode: glassy carbon; reference electrode: SCE.

Wave shape evolutions and the corresponding peak potential locations as a function of pH suggest the influence of protonation to become minimal around pH 5 (Supporting Information, Table S2). Such a trend is observed throughout the whole series of complexes in this work, both for the Fe^{III}/Fe^{II} redox couple and for the tungsten centres. We reasoned that this situation might allow, at least partly, a tentative separation between structural and acid–base influences on the electrochemical behaviours of the present complexes. For this purpose, we focus on some observations related to W waves in pH 5 medium. On the basis of this hypothesis of minimal pH influence, it can be assumed that the changes observed in the CVs of the complexes at pH 5 are mainly due to structural differences that exist between different molecules. We note for example that the addition of two Fe^{III} centres to one molecule of Ni2As4 results in a more pronounced separation between the first two tungsten waves in the daughter molecule Fe2_Ni2As4. The gap between the first two tungsten reduction peak potentials, ΔE (W1 – W2), grows from 132 mV for compound Ni2As4 to 150 mV for Fe2_Ni2As4 (Supporting Information, Table S5). It must be kept in mind that the addition of two Fe^{III} centres on one molecule of Ni2As4 is followed by an internal isomerization that results in the transformation of the αααα-type junction between the two tungsten frameworks and the central metallic cluster to a αββα-type junction. The same isomerization is observed during the transformations Ni2As4 → Ni4AS4, Ni2As4 → FeNi_Ni2As4 and Fe2As4 → Ni2_Fe2As4. In short, it can be concluded that the isomerization from αααα-type to αββα-type junction induces a split of the two first W waves provided the influence of protonation is minimal (Supporting Information, Table S3).

Electrocatalysis

This section summarizes preliminary results obtained during studies conducted on the electrocatalytic properties of the Fe-containing mixed-metal sandwich complexes of this work. A comparative study of the electrocatalytic reduction of nitrite by Fe2As4, Ni2_Fe2As and Fe2_Ni2As4 in a pH 1 medium (0.5 M Li_2SO_4 + H_2SO_4) is presented. Complementary experiments related to Ni2As4 and Ni4As4 in the reduction of NO_2^- are described in the Supporting Information. Finally, dioxygen and hydrogen peroxide reductions were studied at pH 5 (1.0 M $LiCH_3COO$ + CH_3COOH) and the results are reported in the Supporting Information.

Electrocatalysis of the reduction of NO_2^- by POMs was demonstrated in the late 1980s.[50–52] Since then, this reaction has been selected and is being used worldwide as a classical test for the electrocatalytic properties of POMs. The catalytic efficiency is defined as CAT = $100 \times [I(\text{POM} + NO_2^-) - I^d(\text{POM})]/I^d(\text{POM})$, where $I(\text{POM} + NO_2^-)$ is the current for the reduction of the POM in the presence of NO_2^- and $I^d(\text{POM})$ is the corresponding diffusion current for the POM alone. The mechanistic issues of this reaction, likely to be of interest here, had been unravelled in detail for a Fe^{III}-substituted tungstic POM and rely on the intermediate formation of a Fe–nitrosyl derivative.[50] The actual catalytic process yielding ammonia occurs by reduction of this Fe–nitrosyl derivative at more negative potentials where the necessary number of electrons is accumulated and delivered by the W framework. However, it must be kept in mind that redox catalysis and chemical catalysis pathways cannot always be delineated sharply as concerns the electrocatalytic reduction of nitrite and nitric oxide. As a matter of fact, Keita et al.[51,52] demonstrated, at the same time that Anson was establishing the aforementioned mechanism,[50] that this catalytic process is observed with a large variety of POMs, including several plenary unsubstituted ones and even lacunary species. To keep a recent example, a supramolecular compound like $[P_8W_{48}O_{184}]^{40-}$, with only W centres, can also be used to reduce NO efficiently.[48,53]

In the present pH 1 experiments, the two processes $HNO_2 \rightleftarrows H^+ + NO_2^-$, pK_a = 3.3 at 18 °C and 3 $HNO_2 \rightleftarrows HNO_3 + 2\ NO + H_2O$ indicate that nitrous acid might be the reactive intermediate.

Figure 7 compares the CVs, in a pH 1 medium, restricted to Fe^{III} reduction potential domain for Fe2_Ni2As4 and Ni2_Fe2As4 upon addition of nitrite (γ = 30). The positive shift between these CVs (ΔE = +90 mV on onset values) is consistent with the one observed in the absence of nitrite (ΔE = +140 mV on reduction peak potential values) under the same conditions. Surprisingly, the current intensity of the Fe2_Ni2As4 wave appears to be less than half as large as that of Ni2_Fe2As4. Furthermore, comparison of these current intensities with those measured in the absence of nitrite indicates the existence of an electrocatalytic process in the explored potential domain. Such observations are at odd with the expectation of only Fe–nitrosyl formation in

this potential domain. Indeed, Fe^{III} centres in the complex Fe2_Ni2As4 are located in external sites; they are more accessible than internal Fe sites and should, in principle, more easily form Fe–nitrosyl complexes. Among tentative explanations, a possible rationale can be proposed in line with the CVs observed in a pH 1 medium in the absence of nitrite. Taking into account that the reduction of iron centres within Fe2_Ni2As4 is nearly "irreversible" in pH 1 medium, it can be assumed that the formation of Fe–nitrosyl competes with the source of irreversibility. In the framework of the intermediacy of Fe–nitrosyl in this catalytic process, further work based on this hypothesis will be carried out. Meanwhile, it clearly comes out that the catalytic efficiency is closely dependent on the position of iron atoms in the central cluster $Ni_2Fe_2O_{14}(H_2O)_2$. Work in progress will evaluate the influence of the nature, charge and size of the adjacent "d" metal atom on the electrocatalytic properties of Fe^{III} within such POMs in several processes.

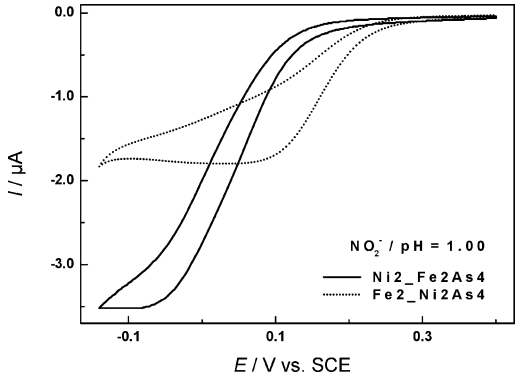

Figure 7. Cyclic voltammograms for the electrocatalytic reduction of nitrite with 0.1 mM POM solutions in a pH 1 medium (0.5 M Li_2SO_4 + H_2SO_4), γ = 30. Ni2_Fe2As4 (solid line) and Fe2_Ni2As4 (dotted line). The scan rate was 2 mV s^{-1}, the working electrode was glassy carbon, and the reference electrode was SCE. The excess parameter γ is defined as $\gamma = C(NO_x)/C(POM)$.

Conclusions

Mixed-metal sandwich-type compounds based on Wells–Dawson fragments $[X_2W_{15}O_{56}]^{12-}$ constitute a novel class of polyoxoanions that has been discovered very recently. Only very few compounds of this type are described and fully characterized. This work has presented the compound $[Na_2(H_2O)_2Ni_2(As_2W_{15}O_{56})_2]^{18-}$, which was synthesized and structurally characterized for the first time by X-ray crystallography. It appears that the presence of Na^+ ions and the pH of the medium (ca. 4.6) are essentials for the formation of disubstituted sandwich-type Dawson polyoxoanions. Therefore, complexes $[Na_2(H_2O)_2M_2(X_2W_{15}O_{56})_2]^{n-}$ (M = Cr, Mn, Co, Ni, Cu, Zn and X = As or P) were obtained pure, with good yields (60–90%). Interestingly these disubstituted species react with a variety of transition-metal centres and lead to a series of mixed-metal-substituted polyoxoanions with even more interesting properties. For example mixed iron–nickel complexes prepared in this study are effective in the electrocatalytic reduction of nitrite, dioxygen and hydrogen peroxide, and present very promising magnetic properties.

Experimental Section

General Methods and Materials: Pure water was used throughout. It was obtained by passing water through a RiOs 8 unit followed by a Millipore-Q Academic purification set. All reagents were of high-purity grade and were used as purchased and without further purification. Elemental analysis was performed by the Service Central d'Analyse CNRS Solaize, France. The IR spectra were recorded as KBr pellets with a Nicolet Magna IR Spectrometer 550 spectrophotometer. Magnetic measurements were carried out on polycrystalline samples by using a SQUID magnetometer, Quantum Design MPMS-5. The UV/Vis spectra were recorded with a Perkin–Elmer Lambda 19 spectrophotometer on 2.5×10^{-5} M solutions of the relevant polyanion. Matched 1.000 mm optical path quartz cuvettes were used. The compositions of the various media were as follows: for pH 1 and 3: 0.5 M Li_2SO_4 + H_2SO_4; for pH 5: 1 M CH_3COOLi + CH_3COOH; for pH 7: 0.5 M Li_2SO_4 + 0.05 M THAM.

X-ray Crystallography: Intensity data collections were carried out with a Siemens SMART three-circle diffractometer for Ni2As4 and a Bruker Nonius X8 APEX 2 diffractometer for FeNi_Ni2As4, each equipped with a CCD bidimensional detector by using a monochromated wavelength λ(Mo-K_α) = 0.71073 Å. The absorption correction was based on multiple and symmetry-equivalent reflections in the data set by using the SADABS program[65] based on the method of Blessing.[57] The structures were solved by direct methods and refined by full-matrix least-squares by using the SHELX-TL package.[66] Ni2As4 and FeNi_Ni2As4 rapidly lose water at room temperature. A single crystal of Ni2As4 was thus mounted in a capillary tube and the data set was collected at 293 K and a single crystal of FeNi_Ni2As4, which is more unstable, was glued in Paraton-N oil and the data set collected at 100 K. In the structure of Ni2As4 there is a discrepancy between the formulae determined by elemental analysis and the formulae deduced from the crystallographic atom list because of the difficulty in locating all the disordered water molecules and counterions. Furthermore, the data sets for Ni2As4 and FeNi_Ni2As4, which contain large voids occupied by solvent molecules, were corrected with the program SQUEEZE, a part of the PLATON package of crystallographic software used to calculate the solvent disorder area and remove its contribution to the overall intensity data.[67] Finally, the structure of FeNi_Ni2As4 was solved in the noncentrosymmetric space group $P1$, because in this space group it was possible to determine the location of the sodium atom and the iron atom, which are disordered on one of the outer sites of the M_4 unit, whereas in the centrosymmetric space group $P\bar{1}$ only an averaged position was observed. Crystallographic data are given in Tables 1 and 2.

Electrochemical Experiments: The same buffer solutions that were used for UV/Vis spectroscopy were used for electrochemistry, with a polyanion concentration of 10^{-4} M. All cyclic voltammograms were recorded at a scan rate of 10 mV s^{-1} unless otherwise stated. The solutions were deaerated thoroughly for at least 30 min with pure argon and kept under a positive pressure of this gas during the experiments. The source, mounting and polishing of the glassy carbon (V25, Carbone Lorraine, France) electrodes has been described.[68] The glassy carbon electrodes had a diameter of 3 mm. The electrochemical set-up was an EG & G 273 A driven by a PC with the M270 software. Potentials are quoted against a saturated

calomel electrode (SCE). The counter electrode was platinum gauze with a large surface area. All experiments were performed at room temperature.

$Na_{18}[Na_2(H_2O)_2Ni_2(As_2W_{15}O_{56})_2]\cdot 41H_2O$: To a suspension of $Na_{12}[As_2W_{15}O_{56}]\cdot 21H_2O$ (10.00 g, 2.24 mmol) in 0.5 M CH_3COONa/0.5 M CH_3COOH (pH 4.6, 80 mL) was added $NiCl_2\cdot 6H_2O$ (0.53 g, 2.23 mmol) in small portions. The solution was heated to 65 °C for about 30 min and filtered while still hot. Solid NaCl (2.0 g) was then added to the light green, clear filtrate, and the solution was placed in a refrigerator (4 °C) overnight. The pale green crystalline material formed was collected by filtration, washed several times with a NaCl saturated solution and dried in open air (7.8 g, 77.8%) corresponding to the product. IR (2% KBr pellet): $\tilde{\nu}$ = 999 (w), 939 (s), 870 (3), 816 (m), 713 (s), 521 (m), 494 (w), 431 (w), 354 (m) cm^{-1}. $Na_{18}[Na_2(H_2O)_2Ni_2(As_2W_{15}O_{56})_2]\cdot 41H_2O$ (8958.58): calcd. As 3.35, W 61.60, Ni 1.31, Na 5.13; found As 3.14, W 57.27, Ni 1.34, Na 5.78.

$Na_{14}[Fe_2(H_2O)_2Ni_2(As_2W_{15}O_{56})_2]\cdot 55H_2O$: To a solution of $FeCl_3\cdot 6H_2O$ (0.22 g, 0.81 mmol) in 1 M NaCl (50 mL) was added Ni2As4 (3.50 g 0.39 mmol, synthesized as described above) in small portions, while stirring and heating at ≈65 °C. The solution was heated for about 30 min and then filtered while still hot. The yellow and clear filtrate was placed in a refrigerator (4 °C) overnight. The pale yellow crystalline material formed was collected by filtration, washed several times with a saturated NaCl solution and dried in open air (2.0 g, 55.7%) corresponding to the product. IR (2% KBr pellet): $\tilde{\nu}$ = 1000 (w), 950 (s), 874 (m), 825 (m), 753 (s), 663 (m), 527 (w), 493 (w), 376 (w), 326 (w) cm^{-1}. $Na_{14}[Fe_2(H_2O)_2Ni_2(As_2W_{15}O_{56})_2]\cdot 55H_2O$ (9184.18): calcd. As 3.26, W 60.05, Fe 1.22, Ni 1.28, Na 3.50; found As 3.25, W 59.51, Fe 1.22, Ni 1.28, Na 3.71.

$Na_{15}[Fe(H_2O)Ni(H_2O)Ni_2(As_2W_{15}O_{56})_2]\cdot 50H_2O$: To a solution of Ni2As4 (3.50 g, 0.39 mmol, synthesized as described above) in 1 M NaCl (50 mL) was added $FeCl_3\cdot 6H_2O$ (0.12 g, 0.44 mmol). The cloudy solution was heated for about 2 h at 65 °C, filtered while still hot and left open to the air at room temperature. After 1 d, the yellow crystals that formed were collected by filtration, washed with a saturated NaCl solution and dried in air (2.06 g, 57.9%). IR (2% KBr pellet): $\tilde{\nu}$ = 996 (w), 946 (s), 876 (m), 815 (m), 766 (m), 523 (w), 493 (w), 435 (w), 356 (w), 330 (w) cm^{-1}. $Na_{15}[Fe(H_2O)Ni(H_2O)Ni_2(As_2W_{15}O_{56})_2]\cdot 50H_2O$ (9120.08): calcd. As 3.29, W 60.48, Ni 1.93, Fe 0.61, Na 3.78; found As 3.21, W 57.73, Ni 1.84, Fe 0.56, Na 4.68.

$Na_{16}[Na_2(H_2O)_2Fe_2(As_2W_{15}O_{56})_2]\cdot 49H_2O$: To a suspension of $Na_{12}[As_2W_{15}O_{56}]\cdot 21H_2O$ (4.50 g, 1.01 mmol) in 0.5 M CH_3COONa/0.5 M CH_3COOH buffer (pH 4.6, 50 mL) was added $FeSO_4\cdot 7H_2O$ (0.28 g, 1.01 mmol) in small portions under vigorous stirring at room temperature. After complete dissolution, the deep green solution was treated with solid NaCl (3.0 g) and kept in the refrigerator. After 24 h at 4 °C the deep green crystalline material that was formed was collected by filtration (4.30 g, 92.7%) and redissolved in 1 M NaCl (50 mL). The solution was heated at 70 °C with continuous stirring. After 3 h, the solution turned gradually from green to a cloudy yellow colour. This solution was filtered several times while still hot to eliminate a very fine yellow precipitate formed during heating. Beautiful yellow crystals that appear during cooling at room temperature were collected by filtration and dried in air (2.70 g, 58.4%). IR (2% KBr pellet): $\tilde{\nu}$ = 995 (w), 950 (s), 878 (m), 833 (m), 725 (m), 518 (w), 497 (w), 353 (w), 317 (w) cm^{-1}.

$Na_{14}[Ni_2(H_2O)_2Fe_2(As_2W_{15}O_{56})_2]\cdot 54H_2O$: To a solution of $NiCl_2\cdot 6H_2O$ (0.05 g, 0.21 mmol) in 1 M NaCl (10 mL) was added Fe2As4 (1.00 g, 0.11 mmol, synthesized as described above) in small portions, while stirring and heating at ≈65 °C. The solution was heated for an additional 30 min, filtered while still hot and left opened at room temperature. After 1 d yellow crystals formed and were collected by filtration, washed with a saturated NaCl solution and dried in air (0.3 g, 32.6%). IR (2% KBr pellet): $\tilde{\nu}$ = 947 (w), 871 (w), 826 (w), 713 (w), 663 (m), 516 (w), 489 (w), 326 (w) cm^{-1}. $Na_{14}[Ni_2(H_2O)_2Fe_2(As_2W_{15}O_{56})_2]\cdot 54H_2O$ (9166.18): calcd. As 3.29, W 60.17, Ni 1.28, Fe 1.22, Na 3.50; found As 3.21, W 57.44, Ni 1.23, Fe 1.21, Na 3.90.

Supporting Information (see footnote on the first page of this article): Brief discussion on syntheses and relative stability in solution; IR and UV/Vis data; complementary data on the electrochemistry and electrocatalytic reduction of NO_2^-, O_2 and H_2O_2.

Acknowledgments

This work was supported by the Centre National de la Recherche Scientifique (UMR 8180, UMR 8182 and UMR 8000), the University of Versailles and the University of Paris XI. I.M.M. thanks Dr. Robertha Howell for helpful discussions.

[1] M. T. Pope (Ed.), *Heteropoly and Isopoly Oxometalates*, Springer, Berlin, **1983**.
[2] M. T. Pope, A. Müller, *Angew. Chem. Int. Ed. Engl.* **1991**, *30*, 34–48.
[3] M. T. Pope, A. Müller (Eds.), *Polyoxometalates: from Platonic Solids to Anti-Retroviral Activity*, Kluwer Academic Publishers, Dordrecht, The Netherlands, **1994**.
[4] C. L. Hill, *Chem. Rev.* **1998**, *98*, 1–389.
[5] M. T. Pope, A. Müller (Eds.), *Polyoxometalate Chemistry: From Topology via Self-Assembly to Applications*, Kluwer Academic Publishers, Dordrecht, The Netherlands, **2001**.
[6] T. Yamase, M. T. Pope (Eds.), *Polyoxometalate Chemistry for Nano-Composite Design*, Kluwer Academic Publishers, Dordrecht, The Netherlands, **2002**.
[7] R. Contant, G. Hervé, *Rev. Inorg. Chem.* **2002**, *22*, 63–111.
[8] D.-L. Long, E. Burkholder, L. Cronin, *Chem. Soc. Rev.* **2007**, *36*, 105–121.
[9] T. J. R. Weakley, H. T. Evans Jr., J. S. Showell, G. F. Tourné, C. M. Tourné, *J. Chem. Soc., Chem. Commun.* **1973**, *4*, 139–140.
[10] R. G. Finke, M. Droege, J. R. Hutchinson, O. Gansow, *J. Am. Chem. Soc.* **1981**, *103*, 1587–1589.
[11] R. G. Finke, M. W. Droege, *Inorg. Chem.* **1983**, *22*, 1006–1008.
[12] H. T. Evans, C. M. Tourné, G. F. Tourné, T. J. R. Weakley, *J. Chem. Soc., Dalton Trans.* **1986**, 2699–2705.
[13] S. H. Wasfi, A. L. Rheingold, G. F. Kokoszka, A. S. Goldstein, *Inorg. Chem.* **1987**, *26*, 2934–2939.
[14] R. G. Finke, M. W. Droege, P. J. Domaille, *Inorg. Chem.* **1987**, *26*, 3886–3896.
[15] C. M. Tourné, G. F. Tourné, F. Zonnevijlle, *J. Chem. Soc., Dalton Trans.* **1991**, 143–155.
[16] N. Casañ-Pastor, J. Bas-Serra, E. Coronado, G. Pourroy, L. C. W. Baker, *J. Am. Chem. Soc.* **1992**, *114*, 10380–10383.
[17] C. J. Gómez-García, E. Coronado, P. Gómez-Romero, N. Casañ-Pastor, *Inorg. Chem.* **1993**, *32*, 89–93.
[18] C. J. Gómez-García, E. Coronado, P. Gómez-Romero, N. Casañ-Pastor, *Inorg. Chem.* **1993**, *32*, 3378–3381.
[19] J. M. Clemente-Juan, E. Coronado, J. R. Galán-Mascarós, C. J. Gómez-García, *Inorg. Chem.* **1999**, *38*, 55–63.
[20] X.-Y. Zhang, C. J. O'Connor, G. B. Jameson, M. T. Pope, *Inorg. Chem.* **1996**, *35*, 30–34.
[21] T. J. R. Weakley, R. G. Finke, *Inorg. Chem.* **1990**, *29*, 1235–1241.
[22] A. M. Khenkin, C. L. Hill, *Mendeleev Commun.* **1993**, 140–141.

[23] C. J. Gómez-García, J. J. Borrás-Almenar, E. Coronado, L. Ouahab, *Inorg. Chem.* **1994**, *33*, 4016–4022.
[24] R. G. Finke, T. J. R. Weakley, *J. Chem. Crystallogr.* **1994**, *24*, 123–128.
[25] X. Zhang, Q. Chen, D. C. Duncan, C. Campana, C. L. Hill, *Inorg. Chem.* **1997**, *36*, 4208–4215.
[26] X. Zhang, Q. Chen, D. C. Duncan, R. J. Lachicotte, C. L. Hill, *Inorg. Chem.* **1997**, *36*, 4381–4386.
[27] M. Rusu, G. Marcu, D. Rusu, C. Rosu, A.-R. Tomsa, *J. Radioanal. Nucl. Chem.* **1999**, *242*, 467–472.
[28] a) L. H. Bi, E.-B. Wang, J. Peng, R. D. Huang, L. Xu, C. W. Hu, *Inorg. Chem.* **2000**, *39*, 671–679; b) L. H. Bi, R. D. Huang, J. Peng, E.-B. Wang, Y.-H. Wang, C.-W. Hu, *J. Chem. Soc., Dalton Trans.* **2001**, 121–129.
[29] U. Kortz, S. Isber, M. H. Dickman, D. Ravot, *Inorg. Chem.* **2000**, *39*, 2915–2922.
[30] X. Zhang, T. M. Anderson, Q. Chen, C. L. Hill, *Inorg. Chem.* **2001**, *40*, 418–419.
[31] a) T. M. Anderson, K. I. Hardcastle, N. Okun, C. L. Hill, *Inorg. Chem.* **2001**, *40*, 6418–6425; b) X. Zhang, C. L. Hill, *Chem. Ind. (London, UK)* **1998**, *75*, 519.
[32] a) L. Ruhlmann, L. Nadjo, J. Canny, R. Contant, R. Thouvenot, *Eur. J. Inorg. Chem.* **2002**, 975–986; b) L. Ruhlmann, J. Canny, R. Contant, R. Thouvenot, *Inorg. Chem.* **2002**, *41*, 3811–3819.
[33] T. M. Anderson, X. Zhang, K. I. Hardcastle, C. L. Hill, *Inorg. Chem.* **2002**, *41*, 2477–2488.
[34] U. Kortz, M. G. Savelieff, B. M. Bassil, B. Keita, L. Nadjo, *Inorg. Chem.* **2002**, *41*, 783–789.
[35] I. M. Mbomekalle, B. Keita, L. Nadjo, P. Berthet, W. A. Neiwert, C. L. Hill, M. D. Ritorto, T. M. Anderson, *Dalton Trans.* **2003**, *13*, 2646–2650.
[36] I. M. Mbomekalle, B. Keita, L. Nadjo, P. Berthet, K. I. Hardcastle, C. L. Hill, T. M. Anderson, *Inorg. Chem.* **2003**, *42*, 1163–1169.
[37] I. M. Mbomekalle, B. Keita, L. Nadjo, W. A. Neiwert, L. Zhang, K. I. Hardcastle, C. L. Hill, T. M. Anderson, *Eur. J. Inorg. Chem.* **2003**, 3924–3928.
[38] L. Ruhlmann, J. Canny, J. Vaissermann, R. Thouvenot, *Dalton Trans.* **2004**, 794–800.
[39] X. Fang, T. M. Anderson, C. Benelli, C. L. Hill, *Chem. Eur. J.* **2005**, *11*, 712–718.
[40] F. Hussain, M. Reicke, V. Janowski, S. de Silva, J. Futuwi, U. Kortz, *C. R. Chim.* **2005**, *8*, 1045–1056.
[41] I. M. Mbomekalle, R. Cao, K. I. Hardcastle, C. L. Hill, M. Ammam, B. Keita, L. Nadjo, T. M. Anderson, *C. R. Chim.* **2005**, *8*, 1077–1086.
[42] T. M. Anderson, X. Fang, I. M. Mbomekalle, B. Keita, L. Nadjo, K. I. Hardcastle, A. Farsidjani, C. L. Hill, *J. Cluster Sci.* **2006**, *17*, 183–195.
[43] a) L. Ruhlmann, C. Costa-Coquelard, J. Canny, R. Thouvenot, *Eur. J. Inorg. Chem.* **2007**, 1493–1500; b) L. Ruhlmann, C. Costa-Coquelard, J. Canny, R. Thouvenot, *J. Electroanal. Chem.* **2007**, *603*, 260–268.
[44] C. P. Pradeep, D.-L. Long, P. Koegerler, L. Cronin, *Chem. Commun.* **2007**, *41*, 4254–4256.
[45] B. Botar, P. Koegerler, *Dalton Trans.* **2008**, 3150–3152.
[46] C. Ritchie, A. Ferguson, H. Nojiri, H. N. Miras, Y.-F. Song, D.-L. Long, E. Burkholder, M. Murrie, P. Kogerler, E. K. Brechin, L. Cronin, *Angew. Chem. Int. Ed.* **2008**, *47*, 5609–5612.
[47] I. M. Mbomekalle, PhD Dissertation, Université Paris-Sud XI, **2003**.
[48] a) B. Keita, L. Nadjo in *Encyclopedia of Electrochemistry: Electrochemistry of Isopoly and Heteropoly Oxometalates* (Eds.: A. J. Bard, M. Stratmann), Wiley-VCH, Weinheim, **2006**, vol. 7, pp. 607–700; b) B. Keita, L. Nadjo, *J. Mol. Catal. A* **2007**, *262*, 190–215.
[49] B. Keita, I. M. Mbomekalle, Y. W. Lu, L. Nadjo, P. Berthet, T. M. Anderson, C. L. Hill, *Eur. J. Inorg. Chem.* **2004**, 3462–3475.
[50] J. E. Toth, F. C. Anson, *J. Am. Chem. Soc.* **1989**, *111*, 2444–2451.
[51] B. Keita, L. Nadjo, R. Contant, M. Fournier, G. Hervé (CNRS), French Patent 89/1, 728, **1989**.
[52] B. Keita, L. Nadjo, R. Contant, M. Fournier, G. Hervé, *Eur. Patent Appl. EP 382*, 644, **1990**; [*Chem. Abst.* **1991**, *114*, 191882u].
[53] B. Keita, F. Girard, L. Nadjo, R. Contant, R. Belghiche, M. Abbessi, *J. Electroanal. Chem.* **2001**, *508*, 70.
[54] J. P. Ciabrini, PhD Dissertation, University Paris VI, **1982**.
[55] Wasfi et al. described the anion $[Fe_4Cu_2W_{18}O_{70}H_6]^{10-}$ (ref.[13]), where a tetrametallic cluster Fe_2Cu_2 is sandwiched between two moieties FeW_9. This compound was obtained by a one-pot synthesis, and even in this case, Fe atoms still occupied the internal positions in the central cluster. So, the idea to get Fe atoms in the external positions is very important. For the first time we have Fe^{III} on the external sites and coordinated to H_2O molecule, its behaviour can be compared with noncoordinated Fe^{III} (when the Fe atoms are in internal positions), case known and described until now.
[56] B. J. Hornstein, R. G. Finke, *Inorg. Chem.* **2002**, *41*, 2720–2730.
[57] R. Blessing, *Acta Crystallogr., Sect. A* **1995**, *51*, 33.
[58] K. Kambe, *J. Phys. Soc. Jpn.* **1950**, *5*, 48.
[59] B. Keita, I. M. Mbomekallé, L. Nadjo, R. Contant, *Electrochem. Commun.* **2001**, *3*, 267–273.
[60] B. Keita, A. Belhouari, L. Nadjo, R. Contant, *J. Electroanal. Chem.* **1998**, *442*, 49–57.
[61] One must take into account that for ionic volume that remains unchange (the total number of atoms is the same in the two complexes Ni2As4 and Fe2_Ni2As4), the overall electrical charge increase for more than 20%, which is very significant if one considers the change in charge density that follows.
[62] In Ni2As4, junctions between the two tungstic fragments, $[As_2W_{15}O_{56}]^{12-}$, and the equatorial metallic cluster $Na_2Ni_2O_{16}$ is from αααα-type. The replacement of the two Na^+ by two Fe^{3+} is accompanied by structural reorganization, which leads to a new type of junction between $[As_2W_{15}O_{56}]^{12-}$ fragments and the new equatorial cluster, $Fe_2Ni_2O_{16}$, a αββα-type junction.
[63] B. Keita, I. M. Mbomekalle, L. Nadjo, T. M. Anderson, C. L. Hill, *Inorg. Chem.* **2004**, *43*, 3257–3263.
[64] S. Romo, J. A. Fernández, J. M. Maestre, B. Keita, L. Nadjo, C. de Graaf, J. M. Poblet, *Inorg. Chem.* **2007**, *46*, 4022–4027.
[65] G. M. Sheldrick, *SADABS*, *Program for Scaling and Correction of Area Detector Data*, University of Göttingen, Germany, **1997**.
[66] G. M. Sheldrick, *SHELX-TL*, *Software Package for the Crystal Structure Determination*, version 5.03, Siemens Analytical X-ray Instrument Division, Madison, WI USA, **1994**.
[67] P. van der Sluis, A. L. Spek, *Acta Crystallogr, Sect. A* **1990**, *46*, 194.
[68] B. Keita, L. Nadjo, *J. Electroanal. Chem.* **1988**, *243*, 87–103.

Received: July 2, 2009
Published Online: October 20, 2009

